

HIERARCHICAL OPTIMIZATION OF THE STRUCTURE AND THE MATERIAL USED IN ITS MANUFACTURE

Pedro G. Coelho^a, Paulo R. Fernandes^b, José M. Guedes^b and Hélder C. Rodrigues^b

^a*DEMI-FCT, UNL, Lisbon, Portugal, pgc@fct.unl.pt*

^b*IDMEC-IST, TU Lisbon, Lisbon, Portugal, prfernan@dem.isi.utl.pt, jmguedes@ist.utl.pt, hcr@ist.utl.pt*

Keywords: Topology, Optimization, Hierarchical, Material, Microstructure.

Abstract. This work addresses the problem of hierarchical topology optimization of structures and its applicability. Assuming that the structure is made of a locally periodic material, and based on the premises of topology optimization of structures, hierarchical topology optimization has the purpose of simultaneously optimize the lay-out of the structure and the material microstructure i.e. its characteristic unit cell. Here the problem is formulated as a structural compliance minimization (stiffness maximization) problem subjected, not only to a global volume upper bound constraint, but also to local material constraints that will guarantee appropriate features for fabrication or requirements in specific applications. The inclusion of (local) material microstructure constraints is critical if one seeks the identification of practical materials designs for instance in the design of bone substitutes (bone grafts). To demonstrate the model developed and its applicability, several examples ranging from structural engineering to biomechanical applications will be presented and discussed.

1 INTRODUCTION

This work addresses the problem of hierarchical topology optimization of structures where the structure and its material are simultaneously optimized and analyses its applicability. The hierarchical topology optimization of structures requires a set of design variables covering two domains; the structure domain (macro or global scale) and the material domain (micro or local scale). A natural scale is associated with each of these domains. At the structure domain, associated with the macroscale, one assumes a material with variable density, as in standard material based topology design formulations. Additionally at the material domain, associated with the microscale, one assumes a cellular/composite designable periodic material.

For this type of multiscale optimization, with compliance minimization and volume constraint, the Optimality Criteria (OC) Method has proved to be a straightforward and computationally efficient method (Bendsoe and Sigmund, 2003; Rodrigues et al., 2002). However, if one introduces design requirements such as local material design constraints (material symmetries, manufacturing details, perimeter or permeability control, etc), a proper algorithmic treatment has to be made since OC is not suitable to handle several constraints. Mathematical programming methods such as the Method of Moving Asymptotes (MMA) (Svanberg, 1987) and Convex Linearization method (CONLIN) (Fleury 1989) have been used successfully in hierarchical topology optimization dealing with extra design constraints (Coelho et al., 2007).

Besides man-made structures, there are natural ones, such as bone or wood, which exhibit a hierarchical structure and for which mathematical models have been developed to understand the fine structural arrangement found at different length scales (Lucchinetti, 2001; Gibson and Ashby, 1988). Here we will present also some applications of the hierarchical optimization model to simulate the natural process of bone adaptation to mechanical loads. The results demonstrate that bone microstructure is not simply mechanically “optimal” but other factors (namely biological ones) play an important role in bone architecture (see e.g. Sigmund, 1999; Coelho et al., 2009). Among these factors one may stress permeability defined as a coefficient that measures quantitatively the ability of a porous medium to conduct fluid flow and implies interconnectivity of the pores, thus playing an important role in the blood flow, cell migration and nutrients diffusion within bone tissue (Nauman et al., 1999; Kohles et al., 2001; Kohles and Roberts, 2002; Martin, 1984). In the formulation presented, bone intertrabecular permeability is taken into account in the remodeling model as a local constraint dependent on relative density (ρ). Results are shown for a three-dimensional model of a proximal femur bone. At macroscale they show a good agreement with physiological relative density distribution. At microscale the resulting microstructures are more convoluted and present a surface distribution qualitatively in agreement with the empirical/experimental curves (Fyhrie et al., 1993; Fyhrie et al. 1995; Coelho et al., 2009).

2 HIERARCHICAL OPTIMIZATION MODEL

As illustrated in figure 1, the model considers a design domain Ω at macroscale level (structural) where the goal is to find an optimal structure topology (lay-out) for given loads (surface tractions \mathbf{t} along Γ_t) and support conditions (imposed displacements \mathbf{u} along Γ_u). At each point \mathbf{x} in Ω , the design model computes a relative density $\rho \in]0, \rho_{\max} \leq 1]$ which defines the structure lay-out. Intermediate values for ρ (gray) mean the existence of a cellular material defined at microscale level. At this level the aim is to find the optimal design of the material unit cell from which the structure is manufactured. This cell is assumed to be periodically repeated inside a small neighborhood of each point $\mathbf{x} \in \Omega$. This periodicity is only

local since unit cell topology may vary with the macroscopic variable \mathbf{x} although smooth transitions must be assumed. Furthermore, it is assumed that the two scales differ by a proper size ratio, *i.e.* the material unit cell characteristic size, d , is much smaller than the characteristic size of the global domain D .

The material unit cell geometry is defined by the “micro” density $\mu \in]0,1]$ function of \mathbf{y} in the design domain Y ($|Y|=1$) for fixed \mathbf{x} in Ω . Here intermediate values for μ are not physically justified so they are penalized through SIMP (Solid Isotropic Model with Penalization) to warrant well-defined microstructures.

In summary, a two-scale material distribution problem (macro and micro) is defined and a “density” field governs each one, $\rho(\mathbf{x})$ and $\mu(\mathbf{y})$, respectively. The interpolation schemes between material properties and density used at macro and micro scales are the homogenization method and SIMP, respectively.

For compliance objective function, the multiscale topology optimization problem, for multiloading with P load cases, can be formulated as:

$$\max_{\substack{\rho(\mathbf{x}) \\ 0 \leq \rho(\mathbf{x}) \leq \rho_{\max} \\ \int_{\Omega} \rho(\mathbf{x}) d\Omega \leq V^*}} \min_{\substack{\mathbf{u}^r \in U \\ r=1, \dots, P}} \left[\int_{\Omega} \Phi(\rho, \mathbf{u}^1, \dots, \mathbf{u}^P) d\Omega - \sum_{r=1}^P \alpha^r \left(\int_{\Omega} \mathbf{b}^r \cdot \mathbf{u}^r d\Omega + \int_{\Gamma_T^r} \mathbf{t}^r \cdot \mathbf{u}^r ds \right) \right] \quad (1)$$

with the optimal energy density function $\Phi(\rho, \mathbf{u}^1, \dots, \mathbf{u}^P)$ solution of the local (micro) optimization problem,

$$\Phi(\rho, \mathbf{u}^1, \dots, \mathbf{u}^P) = \max_{\substack{\mu(\mathbf{y}) \\ 0 \leq \mu(\mathbf{y}) \leq 1 \\ \int_Y \mu(\mathbf{y}) dY = \rho(\mathbf{x}) \\ g[\mu(\mathbf{y})] = g^*[\rho(\mathbf{x})]}} \sum_{r=1}^P \alpha^r \left[\frac{1}{2} E_{ijkl}^H(\mu) \epsilon_{ij}(\mathbf{u}^r) \epsilon_{kl}(\mathbf{u}^r) \right] \quad (2)$$

The max-min problem (1) is equivalent to a compliance minimization problem. This is the global problem related with the macroscopic spatial distribution of material in Ω subjected to a resource volume constraint V^* . Problem (2) is the point wise maximization of the strain energy density function for the strain fields $\boldsymbol{\epsilon}$. The elasticity tensor superscript “H” denotes the homogenized properties of the cellular material. This is the local anisotropy material distribution problem subjected to a prescribed material volume fraction and to an extra material design constraint function g evaluated for a local design, μ , and its value should meet a target g^* that in turn depends on global design variables, ρ . For a detailed description see Rodrigues et al., (1999) and Bendsoe and Sigmund, (2003).

3 ALGORITHMIC STRATEGY

Some algorithmic strategies have been applied to efficiently solve problem (1-2) (Coelho et al., 2007). The optimality criteria based methods solve the optimality conditions following basically a fix-point type update scheme for the density. Although these methods proved to be easy for numerical implementation and quite efficient in applications with a single constraint (usually a total volume constraint), the same is not verified in the case of multiple constraints. In order to broaden hierarchical optimization applicability, especially when local design constraints are imposed, it is critical to find appropriate algorithmic strategy.

The algorithmic strategy adopted here considers both the macro (global) and micro (local) densities as independent design variables and therefore each problem (global/local) may have its own optimizer. It combines Method of Moving Asymptotes (MMA) to solve (1) with

Convex Linearization method (CONLIN) to solve (2). CONLIN is used here as the local optimiser since it gives the correct Lagrange multipliers, essential to satisfy the optimality conditions.

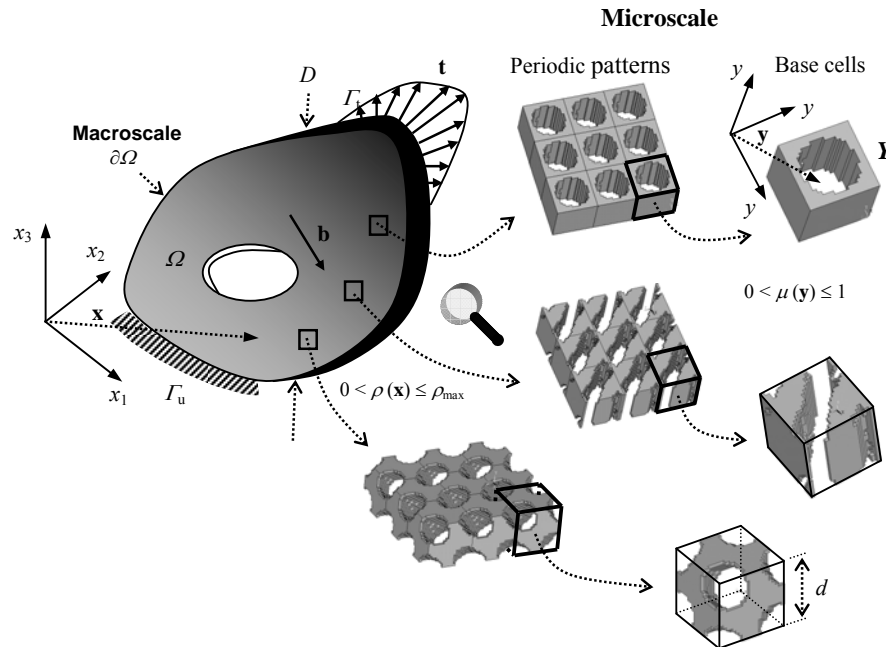


Figure 1: Material model used in two-scale topology optimization

The necessary condition for the inner *min* problem in (1) is just the equilibrium condition (in weak form) and is satisfied for the actual displacement fields. Thus one can rewrite (1) as

$$\max_{\substack{\rho(x) \\ 0 \leq \rho(x) \leq 1 \\ \int_{\Omega} \rho(x) d\Omega \leq V^*}} \left(- \int_{\Omega} \Phi(\rho, u^1, \dots, u^P) d\Omega \right) \quad (3)$$

where \mathbf{u}^r , $r = 1, \dots, P$, is the actual displacement field for the r^{th} load case.

Since maximization in (3) with respect to (*w.r.t.*) design variable ρ is solved by a mathematical programming method one needs gradient information of $\Phi(\rho)$ *w.r.t.* the density variable ρ .

From problems (1, 2) and since ρ is a resource constraint bound in problem (2) one gets the gradient given as (see e.g. Coelho et al., 2008):

$$\frac{\partial \Phi}{\partial \rho} = \lambda_1 + \lambda_2 \frac{\partial g^*(\rho)}{\partial \rho} \quad (4)$$

where λ_1 and λ_2 are the Lagrange Multipliers for the resource and $g(\cdot)$ constraints respectively in (2)

If (2) has only the resource constraint then the derivative of Φ in (4) is simply equal to the respective Lagrange multiplier λ .

The gradient related to problem (2) *w.r.t.* μ is derived analytically yielding:

$$\frac{1}{2} \left\langle \frac{\partial E_{ijkl}^H(\mu)}{\partial \mu}, \partial \mu \right\rangle \varepsilon_{ij}(\mathbf{u}^r) \varepsilon_{kl}(\mathbf{u}^r) \tag{5}$$

Expressions (4) and (5) are valid only for intermediate values of macro and micro densities, respectively (the interested reader is referred to Coelho et al., 2008 where a detailed development is presented).

4 COMPUTATIONAL PROCEDURE

The two-scale model (see figure 1 and problems (1) and (2)) implies the iterative solution of one problem at a global (or macro) scale and many problems at a local (or micro) scale characterizing the material microstructure. Here, one considers as many local problems as the number of the finite elements used in the global mesh (macroscale). Since the local optimization problems can be independently solved, the model can be efficiently solved by computational means using parallel computing techniques (see Coelho et al., 2007, 2010). Between two consecutive iterations on global problem, local problems are distributed among several processors to speed up the local solutions task. Plots of speed-up and efficiency curves using some processors were obtained and presented in (Coelho et al. 2010) showing a very good scalability for this problem.

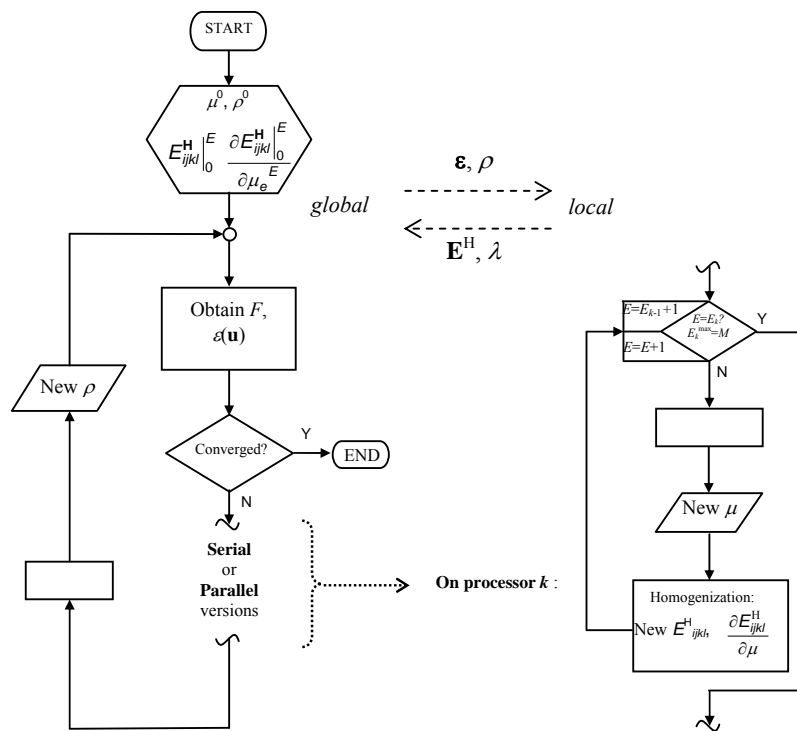


Figure 2: Flowchart for the MMA/CONLIN algorithmic strategy

In figure 2 it is shown, by means of a flowchart, the computational procedure to run the algorithmic strategy MMA/CONLIN in a parallel computing environment. The dashed arrows represent the main data flow between global and local problems.

5 APPLICATION IN STRUCTURAL DESIGN

This example considers a supported beam subjected to a multiple load condition (two loads not simultaneously applied) as shown in figure 3a. Through this example it is analysed the influence of the shear and bending loads in the design. The problem was solved with 588 finite elements for the global problem while the local problem was solved with a 20x20x20 mesh.

The volume constraint considered is 35% of the total volume of the design domain. It is assumed a base material E_{ijkl}^0 linear and isotropic. The material properties are 210 GPa for Young's Modulus and 0.3 for Poisson ratio. The final global material distribution is presented in figure 3b.

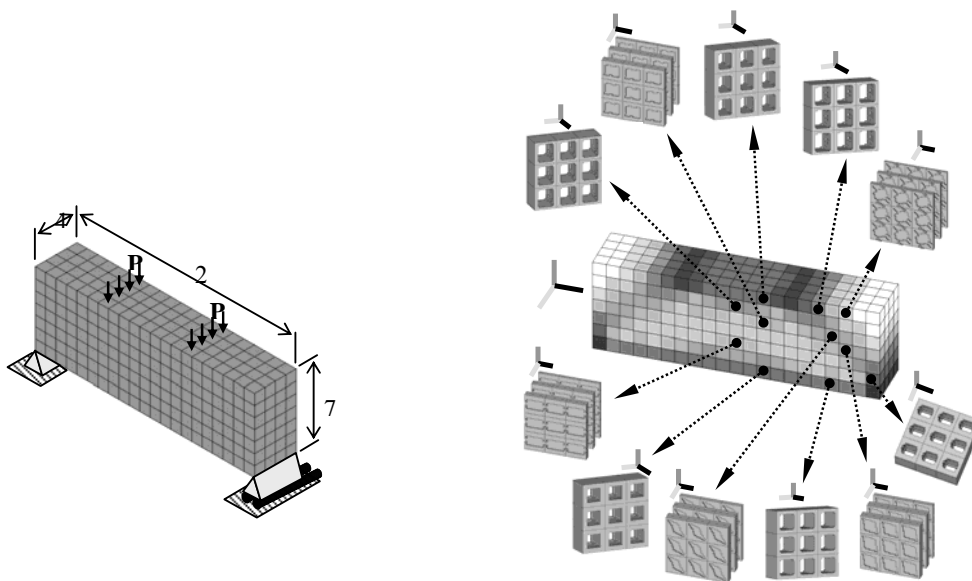


Figure 3: (a) Example definition, (b) Macro density field and some microstructures

6 APPLICATION TO BONE REMODELING

Since the observations of Wolff, generally called the Wolff's Law (Wolff, 1892), several mathematical and computational models for bone functional adaptation have been developed. Among these models the hierarchical model (see e. g. Rodrigues et al., 1999, Coelho et al., 2009) appears as one of the most interesting developments.

All models agree on the fact that the local mechanical environment plays a crucial role in this natural adaptation process. However it has been observed that the structure obtained by simple stiffness maximization doesn't agree in various biologically driven features present in real bone, namely porosity, permeability and surface area density (see e.g. Sigmund, 1999; Coelho et al. 2009). In this section the consequences of these biological features are analyzed through the introduction of a permeability constraint at the local level and thus showing the hierarchical model capability to treat local constraints at the microstructure level.

6.1 Permeability constraint

Microstructure permeability will be enforced introducing, in the optimal design problem (2), a lower bound local constraint $g^*(\rho) - g(\mu) \leq 0$. The function $g(\mu)$ is defined based on

components from the homogenized permeability tensor \mathbf{K}^H , (see e.g.) and $g^*(\rho)$ is its lower admissible limit. More specifically we enforce an orthotropic symmetry of the permeability tensor \mathbf{K}^H , imposing the lower limit only to the diagonal components of this tensor and setting equal to zero de off diagonal terms i.e., $K_{ii} \geq K_{\min}$ and $K_{ij, i \neq j} = 0$.

Several curves f_i plotted in figure 4, defining a minimum permeability K_{\min} , are analyzed to study the influence of the respective local design constraint and to gain insight about how close the numerical results are from the real trabecular bone properties.

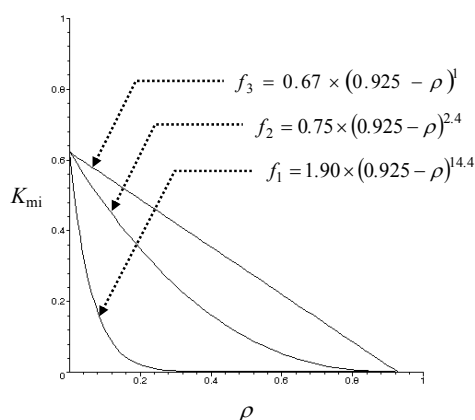


Figure 4: Test curves for the minimum permeability imposed.

6.2 Results

The bone (domain Ω) geometry is based on the standardized femur (Viceconti et al., 2001). The femur bone domain Ω and cell domain Y are discretized by 2112 and 8000 ($20 \times 20 \times 20$) hexahedral isoparametric finite elements with 8 nodes, respectively. Within each finite element Ω^E and Y^e the densities ρ and μ are assumed constant, respectively. It is assumed a solid and isotropic base material defined by 20 GPa of Young's Modulus and 0.3 of Poisson's ratio. The global volume fraction constraint requirement is 50% (for a full description see Coelho et al., 2009).

Physiological loading conditions were assumed as a multiload case (number of load cases, $P = 10$) based on the data reported in Bergmann et al. (2001).

The obtained results for apparent (relative) density distribution and respective microstructures are shown in figure 5. At macroscale level the differences on density distribution obtained with the different permeability limits (figure 3) are minimal. Figures 5a, (obtained for $K_{\min} = f_2$) shows that apparent density distribution reproduces important characteristics of a real femur such as the external compact bone layer (black), the medullar cavity and the less dense spongy bone in the femoral head with the well known Ward's triangle.

At microscale the effect of permeability control is more notorious. Figures 5a identifies some selected elements from different anatomic regions of the femur. The corresponding microstructures with and without permeability control are shown in figure 5c and 5b respectively. Comparing these microstructures it is apparent that permeability control leads to more convoluted solutions resembling better real trabecular bone architecture (e.g. compare microstructures for element 2). In general, without permeability control local solutions tend to exhibit a lack of connectivity (e.g. laminates 2, 3, 9) whereas prescribing a minimum permeability the connectivity property seems to be improved.

Still about the microstructures shown it is worth noting how design/volume fraction differs depending on anatomic site, which is a characteristic of trabecular bone depending on the local stress field. In regions where a triaxial state of stress is dominant the microstructures are equiaxed (closest to isotropic behavior, see *e.g.* element 7, 8). On the other hand there are regions where microstructures are strongly oriented. For uniaxial and biaxial stress fields the resulting microstructures become like honeycomb (see elements 1, 12) or parallel plates (see elements 2, 3). These results agree well with bone microstructure idealizations presented by other authors (see Gibson and Ashby, 1988).

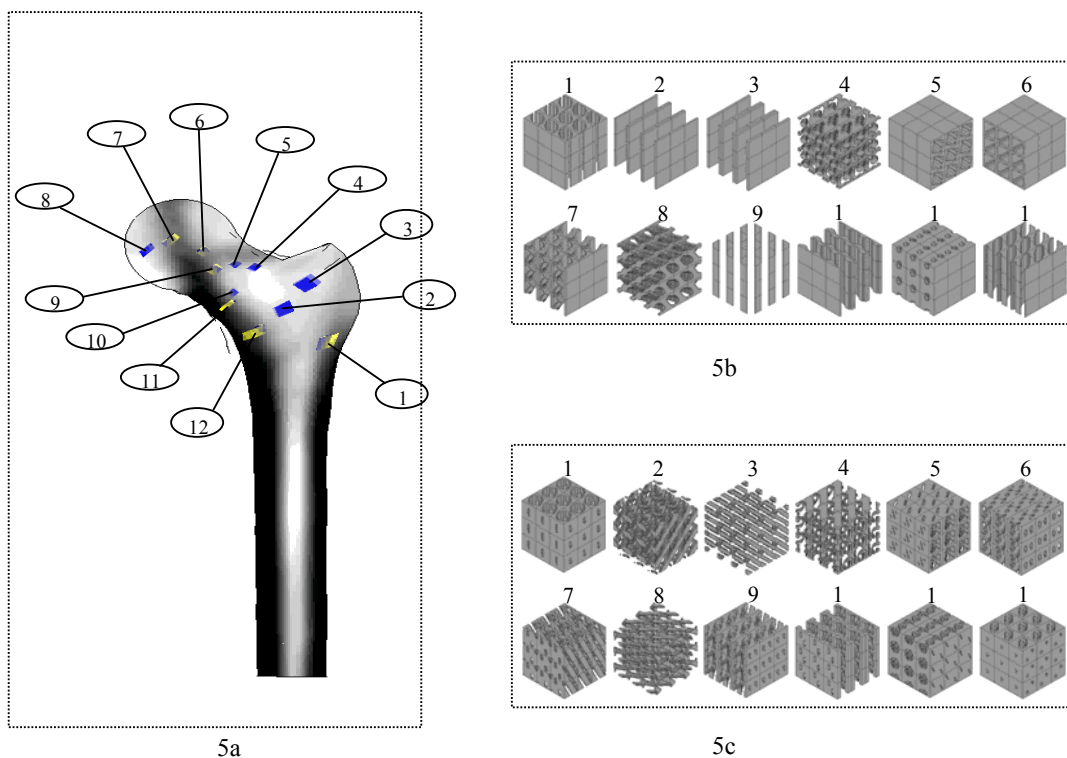


Figure 5: a) Density distribution with local permeability constraint (with function f_2 , see figure 4) and finite element selection for microstructure inspection; b) microstructures obtained without permeability control; c) microstructures obtained with permeability control..

One interesting aspect is observed from the plot of volume fraction result versus bone surface area density (Fyhrie et al., 1993) for each finite element in global mesh.

When the minimum permeability required is very low or absent it is seen that the points are scattered around two curves (see figure 6a), a plateau and an inverted parabola branch. This distribution trend is comparable to results obtained by models assuming simple microstructures for trabecular bone characterization (rod, plate, plate and rod, 3D rod, spherical hole, see *e.g.* Parfitt, 1983). However, bone architectures are not simply parallel plates, in fact they are “perforated plates” linked through small “bars”. These effects appear when the permeability lower limit is increased as seen in figure 4c. As the minimum permeability limit increases (from f_1 to f_3 , see figure 4) the bone surface area density plots (see figures 6a to 6c) approach the distribution observed in real bone (as reported by Martin, 1984) as shown in figure 6d.

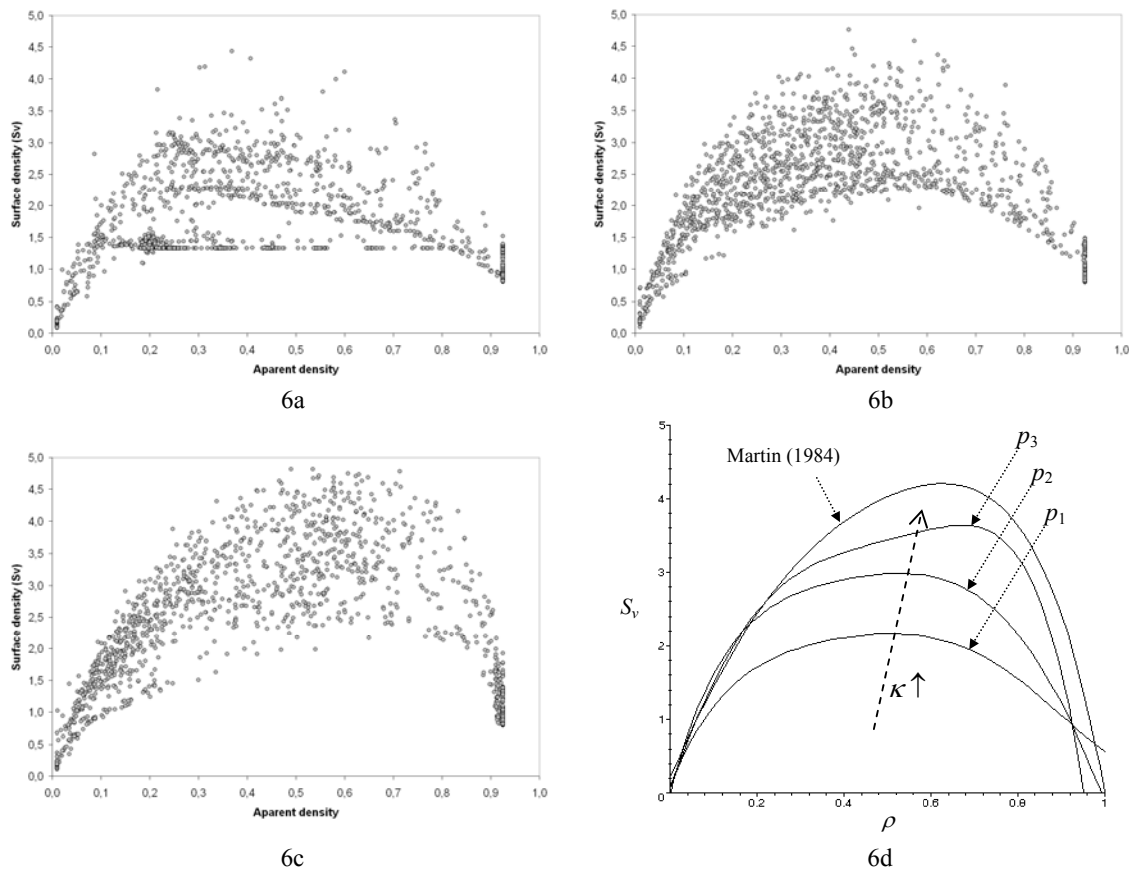


Figure 6: Plotting bone surface area density [mm^2/mm^3] versus apparent density. Results obtained with: a) function f_1 ; b) function f_2 ; c) function f_3 ; d) polynomial interpolation p_1, p_2, p_3 for the results with f_1, f_2, f_3 , respectively.

7 CONCLUSIONS

The main contribution of the present work is to show the wide applicability of hierarchical topology optimization when one includes local design constraints, especially material design constraints. Hierarchical topology optimization leads to massive computations but the independence of local problems favors the use of parallel computing techniques leading to a high reduction of computational time.

The practical interest of hierarchical topology optimization subjected to constraints on material design was shown in several structural applications.

Of special interest is the gain on understanding the fine structure of natural hierarchical materials such as bone. Considering two scales of bone (macro and micro scales related with whole bone and trabecular bone, respectively), the hierarchical model was applied with an extra design constraint that approaches trabecular bone in terms of permeability. This was carried out through microstructure permeability evaluation (homogenized coefficients). The results show a better agreement with real bone when permeability is controlled. As a conclusion, the present hierarchical model allows the evaluation of the relative influence of mechanical stimulus on biologically-driven variables such as the intertrabecular permeability.

ACKNOWLEDGEMENTS

This work was supported by Portuguese foundation for Science and Technology through the project PTDC/EME-PME/71436/2006 and PTDC/EME-PME/67658/2006. The results presented here were produced using the IST Cluster (IST/Portugal).

REFERENCES

- Bendsøe M.P. and Sigmund O. *Topology Optimization: Theory, Methods and Applications*, Springer-Verlag, Berlin, 2003.
- Bergmann G., Deuretzbacher G., Heller M., Graichen F., Rohlmann A., Strauss J. and Duda G., Hip contact forces and gait patterns from routine activities, *Journal of Biomechanics*, 34:859-871,2001.
- Coelho P. G., Fernandes P. R., Guedes J.M. and Rodrigues H.C., Algorithmic strategies for the hierarchical topology optimization of structures. Proc. of WCSMO-07, Seoul, South-Korea, 2007.
- Coelho P.G., Fernandes P.R., Guedes J.M. and Rodrigues H.C., A hierarchical model for concurrent material and topology optimization of three-dimensional structures, *Struct Multidisc Optim*, 35:107-115, 2008.
- Coelho P.G., Fernandes P.R., Rodrigues H.C., Guedes J.M., Cardoso J.B., Numerical modeling of bone tissue adaptation – A hierarchical approach for bone apparent density and trabecular structure, *J. of Biomechanics*, 42(7):830-837, 2009.
- Coelho, P.G., Cardoso, J.B., Fernandes, P.R., and Rodrigues, H.C., Parallel Computing Techniques Applied to the Simultaneous Design of Structure and Material, *Computers & Structures*, 2010 (in print).
- Fazzalari N.L., Crisp D.J. and Vernon-Roberts B., Mathematical modeling of trabecular bone structure: the evaluation of analytical and quantified surface to volume relationships in the femoral head and iliac crest, *J. Biomechanics*, 22:901-910, 1989.
- Fleury C., First and second order convex approximation strategies in structural optimization, *Structural Optimization*, 1:3-10, 1989.
- Fyhrie D.P., Fazzalari N.L., Goulet R. and Goldstein S.A., Direct calculation of the surface-to-volume ratio for human cancellous bone, *J. Biomechanics*, 26:955-967, 1993.
- Fyhrie D.P., Lang S.M., Hoshaw S.J., Shaffler M.B. and Kuo R.F., Human Vertebral Cancellous bone surface distribution, *Bone*, 17:287-291, 1995.
- Gibson L. and Ashby M., *Cellular Solids, Structure and Properties*, Oxford, England: Pergamon Press, 1988.
- Kohles S.S, Roberts., J.B., Upton M.L., Wilson C.G., Bonassar L.J., and Schlichting A.L. Direct perfusion measurements of cancellous bone anisotropic permeability. *J. Biomechanics*, 34: 1197-1202, 2001.
- Kohles S.S. and Roberts J.B., Linear poroelastic cancellous bone anisotropy: trabecular solid elastic and fluid transport properties. *J. Biomech. Eng.*, 124:521-526, 2002.
- Lucchinetti E. Composite model of bone properties. In: Cowin S C (Eds), *Bone Mechanics Handbook. 2nd ed.* CRC Press, 2001.
- Martin R.B., Porosity and specific surface of bone, *CRC Crit Rev biomed Engng*, 10:179-222,1984.
- Nauman E. A., Fong K.E. and Keaveny T.M., Dependence of intertrabecular permeability on flow direction and anatomic site. *Annals of Biomedical Engineering*, 27: 517-524, 1999.
- Parfitt A.M., Mathews C.H., Villanueva A.R., Kleerekoper M., Frame B. and Rao D.S., Relationships between surface, volume, and thickness of iliac trabecular bone in aging and in osteoporosis, *J Clin Invest*, 72:1396-1409, 1983.

- Rodrigues H., Jacobs C., Guedes J. and Bendsoe M. Global and local material optimisation applied to anisotropic bone adaptation. In Proc. of IUTAM Symposium on Synthesis in Bio Solid Mechanics, Copenhagen, Denmark, 221-233, 1999.
- Rodrigues H.C., Guedes J.M. and Bendsoe M.P. Hierarchical optimization of material and structure, *Struct Multidisc Optim*, 24, 1-10, 2002.
- Sigmund, O., On the optimality of bone structure. Proc. of IUTAM Symposium on Synthesis in Bio Solid Mechanics, Copenhagen, Denmark, 221-233, 1999.
- Svanberg K. The method of moving asymptotes – a new method for structural optimization, *Int J Num Meth in Eng*, 24:359-373, 1987.
- Viceconti M., Casali M., Massari B., Cristofolini L., Bassini S. and Toni A., The “standardized femur program” proposal for a reference geometry to be used for the creation of finite element models of the femur, *Journal of Biomechanics*, 29(9):1241, 1996.
- Wolff J., *The Law of Bone Remodeling*. Berlin Heidelberg New York: Springer, 1986 (translation of the German 1892 edition)